 CMES, vol.61, no.2, pp.155-175, 2010

An Efficient Trefftz-Based Method for Three-Dimensional Helmholtz Problems in Unbounded Domains

Bart Bergen[1], Bert Van Genechten[1], Dirk Vandepitte[1] and Wim Desmet[1]

Abstract: The Wave Based Method (WBM) is a numerical prediction technique for Helmholtz problems. It is an indirect Trefftz method using wave functions, which satisfy the Helmholtz equation, for the description of the dynamic variables. In this way, it avoids both the large systems and the pollution errors that jeopardize accurate element-based predictions in the mid-frequency range. The enhanced computational efficiency of the WBM as compared to the element-based methods has been proven for the analysis of both three-dimensional bounded and two-dimensional unbounded problems. This paper presents an extension of the WBM to the application of three-dimensional acoustic scattering and radiation problems. To this end, an appropriate function set is proposed which satisfies both the governing Helmholtz equation and the Sommerfeld radiation condition. Also, appropriate source formulations are discussed for relevant sources in scattering problems. The accuracy and efficiency of the resulting method are evaluated in some numerical examples, including the 3D cat's eye scattering problem.

Keywords: Trefftz, Wave Based Method, mid-frequency, numerical acoustics, scattering

1 Introduction

The efficient solution of Helmholtz problems in unbounded domains, encompassing acoustic or electromagnetic scattering and radiation, is the subject of substantial research effort. Based on the target ratio of the wavelength (λ) and the problem specific dimension (a), the currently available techniques can be roughly divided into two philosophies:

- $\lambda/a \approx 1$**:** These methods are based on a 'low-frequency' approach where geometric detail is relatively important and small compared to the considered wavelengths.

[1] K.U.Leuven, dept. of Mechanical engineering, division PMA, Heverlee, Belgium. Email: bart.bergen@mech.kuleuven.be

- $\lambda/a << 1$**:** These methods are based on a 'high-frequency' approach: the problem geometry is large as compared to the considered wavelengths.

For many practical problems, however, a mid-frequency 'twilight zone' exists, where neither of these philosophies yields an appropriate solution method.

Looking at the low-frequency side, the most generally established methods are the element-based methods. The Finite Element Method (FEM) [Zienkiewicz, Taylor, and Zhu (2005)] discretizes the entire problem domain into a large but finite number of small elements. Within these elements, the dynamic response variables are described in terms of simple, polynomial shape functions. Because the FEM is based on a discretization of the problem domain into small elements, it cannot inherently handle unbounded problems. An artificial boundary is needed to truncate the unbounded problem into a bounded problem. Special techniques are then required to reduce spurious reflection of waves at the truncation boundary. Three strategies are applied to this end [Thompson (2006)]: absorbing boundary conditions [Patlashenko and Givoli (2000)], infinite elements [Bettess (1992)] and absorbing layers [Lu and Zhu (2007)]. Amongst these techniques, especially the derivation of localized higher-order ABC's and the development of efficient Perfectly Matched Layers (PML) are subject of substantial recent research efforts [Givoli (2008)]. A second important element-based technique, the Boundary Element Method (BEM) [Von Estorff (2000)], is based on a boundary integral formulation of the problem. As a result, only the boundary of the considered domain has to be discretized. Within the applied boundary elements, the acoustic boundary variables are expressed in terms of simple, polynomial shape functions, similar to the FEM. Since the boundary integral formulation inherently satisfies the Sommerfeld radiation condition, the BEM is particulary suited for the treatment of problems in unbounded domains.

As the problem wavelengths shorten, the discretization size required in those methods becomes almost exclusively dependant on the considered frequency: an increasingly fine mesh is needed to match the spatial resolution of the response and keep pollution errors [Bouillard and Ihlenburg (1999)] controlled. The resulting large numerical models restrict the practical applicability of these methods to low-frequency problems due to the prohibitively large computational cost [Yue and Guddati (2005); Marburg (2002)].

From the high-frequency side, several techniques are available to study scattering and radiation problems [Chandler-Wilde and Graham (2009); Bleszynski, Bleszynski, and Jaroszewicz (2004)]. A common point in many of these techniques is the separation of the phase from the solution field. In the High-Frequency Boundary Element Method (HF-BEM) [Chandler-Wilde and Graham (2009)], the high fre-

quency asymptotic solution of the problem is used to separate the phase from the scattered field. The remaining problem is then smooth and has a relatively low spatial variation, making it suitable for element-based discretization. Evaluation of the system matrix in such a HF-BEM method still requires the evaluation of highly oscillatory integrals, motivating the development of specialized integration techniques for highly oscillatory kernels [Huybrechs and Vandewalle (2006)]. In ray-tracing methods [Glassner (1989)], the phase information is omitted from the solution and the problem is instead considered in terms of energy propagation. While the resulting technique can be very efficient for high-frequency problems, the lack of accurate phase information poses a limit to the applicability for many practical problems.

In general, the accuracy of those high-frequency methods starts to suffer when considering problems at lower frequencies, where the assumptions made regarding to the phase of the solution break apart. The relatively smaller geometrical detail leads to increased interference and resonances in the solution which can not be accurately captured using the high-frequency assumptions.

Both from the low- and high-frequency side, substantial research effort is spent in extending the application range into the mid-frequency domain. For the low-frequency methods, one common path is the enhancement of the efficiency of the method, thus allowing calculation of more refined and accurate models. A second approach is the incorporation of *a priori* knowledge about the problem into the system, yielding a multitude of enhanced FE/BE methods. For an overview on advances in these methods the reader is referred to Thompson (2006); Bettess (2004); Harari (2006), and the works by Qian, Han, Ufimtsev, and Atluri (2004); Callsen, Von Estorff, and Zaleski (2004); He, Lim, and Lim (2008); Takei, Yoshimura, and Kanayama (2009). Noteworthy in this regard are the so-called Trefftz methods [Trefftz (1926)], where the basis functions are chosen to satisfy the problem equations *a priori*. Based on this principle, several enhanced techniques are devised, tackling various problems including wave scattering. Examples can be found in Sladek, Sladek, Kompis, Van Keer (2000); Cho, Golberg, Muleshkov and Li (2004); Young and Ruan (2005); Li, Lu, Huang and Cheng (2007); Trevelyan and Coates (2010). For the high-frequency methods, several techniques are proposed to enhance the mid-frequency accuracy, e.g. by including a detailed refraction description and better phase models. An overview is given by Chandler-Wilde and Graham (2009).

The Wave Based Method (WBM) [Desmet (1998)] is an alternative modeling technique following the first philosophy, but conceived to offer the enhanced efficiency and low pollution error needed for accurate mid-frequency predictions. To this end, the method is based on an indirect Trefftz approach, using wave functions, which exactly satisfy the governing differential equation, to describe the dynamic

response variables. In this way no approximation error is made inside the problem domain. However, the wave functions may violate the boundary and continuity conditions. Enforcing the residual boundary and continuity errors to zero in a weighted residual scheme yields a small matrix equation which can be solved for the unknown contribution factors of the wave functions used in the expansion of the dynamic field variables. This approach has been applied successfully for many steady-state structural dynamic problems [Vanmaele, Vandepitte, and Desmet (2007, 2009)], both two-dimensional (2D) [Pluymers, Van Hal, Vandepitte, and Desmet (2007); Van Genechten, Vergote, Vandepitte, and Desmet (2010)] and three-dimensional (3D) [Desmet, Van Hal, Sas, and Vandepitte (2002); Van Genechten, Vandepitte, and Desmet (2010)] interior acoustic and vibro-acoustic problems, and 2D exterior (vibro-)acoustic problems [Pluymers, Desmet, Vandepitte, and Sas (2005); Van Genechten, Bergen, Vandepitte, and Desmet (2010)]. It has been shown that, due to the small model size and the enhanced convergence characteristics, the WBM has a superior numerical performance as compared to the element-based methods. As a result, problems at higher frequencies may be tackled.

This paper proposes the necessary tools for applying the WB modeling framework to 3D problems in unbounded domains. After a short problem description in the first section, the WB modeling process is detailed. To use the WBM for unbounded problems, the problem domain is first divided into a bounded and an unbounded part by introducing a truncation sphere. A suitable function set is proposed to efficiently model the outgoing waves in this unbounded region. Combined with the available functions for 3D bounded problems, a model for the total problem is obtained. The resulting technique is finally validated in two numerical case studies, illustrating both the efficiency and accuracy of the proposed approach.

2 Problem description

Consider a general unbounded acoustic problem as shown in figure 1. The steady-state acoustic pressure inside the problem domain is governed by the inhomogeneous Helmholtz equation:

$$\nabla^2 p(\underline{r}) + k^2 p(\underline{r}) = \mathscr{F}(\underline{r}) \tag{1}$$

with ω the circular frequency and $k = \omega/c$ the acoustic wave number. The acoustic fluid is characterised by its density ρ_0 and speed of sound c. The fluid is excited by a source $\mathscr{F}(\underline{r})$. The problem boundary Γ constitutes 2 parts: the finite part of the boundary, Γ_b, and the ficticious boundary at infinity, Γ_∞. Based on the three types of commonly applied acoustic boundary conditions, the finite boundary can

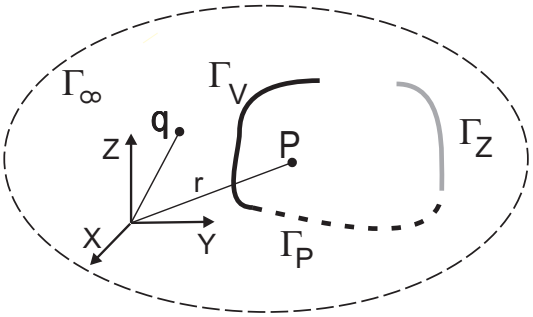

Figure 1: An unbounded acoustic problem

be further divided in three non-overlapping parts: $\Gamma_b = \Gamma_v \cup \Gamma_p \cup \Gamma_Z$. If we define the velocity operator $\mathscr{L}_v(\bullet)$ as:

$$\mathscr{L}_v(\bullet) = \frac{j}{\rho_0 \omega} \frac{\partial \bullet}{\partial n}, \tag{2}$$

we can write the boundary condition residuals:

$$\underline{r} \in \Gamma_v : \qquad R_v = \mathscr{L}_v(p(\underline{r})) - \overline{v}_n(\underline{r}) = 0 \,, \tag{3}$$

$$\underline{r} \in \Gamma_p : \qquad R_p = p(\underline{r}) - \overline{p}(\underline{r}) = 0 \,, \tag{4}$$

$$\underline{r} \in \Gamma_Z : \qquad R_Z = \mathscr{L}_v(p(\underline{r})) - \frac{p(\underline{r})}{\overline{Z}_n(\underline{r})} = 0 \,, \tag{5}$$

where the quantities $\overline{v}_n$, $\overline{p}$ and $\overline{Z}_n$ are, respectively, the imposed normal velocity, pressure and normal impedance. At the boundary at infinity, Γ_∞, the Sommerfeld radiation condition for outgoing waves is applied. This condition ensures that no acoustic energy is reflected at infinity and is expressed as

$$\lim_{|\underline{r}| \to \infty} \left(\underline{r} \Big(\frac{\partial p(\underline{r})}{\partial |\underline{r}|} + jkp(\underline{r}) \Big) \right) = 0 \,. \tag{6}$$

Solution of the Helmholtz equation (1) together with the associated boundary conditions (3), (4), (5) and (6) yields a unique dynamic acoustic pressure field $p(\underline{r})$.

3 The Wave Based Method for acoustic radiation problems

The WBM [Desmet (1998)] is a numerical modeling method based on an indirect Trefftz approach for the solution of steady-state acoustic problems in both bounded

and unbounded problem domains. Instead of using simple approximating polynomials like in the FEM or BEM, the field variables are expressed as an expansion of wave functions, which inherently satisfy the governing equation, in casu the Helmholtz equation (1). The degrees of freedom are the weighting factors of the wave functions in this expansion. It is an indirect approach, since these weighting factors are not the dynamic field variables themselves. Enforcing the boundary and continuity conditions using a weighted residual formulation yields a system of linear equations whose solution vector contains the wave function weighting factors.

The general modeling procedure consists of the following steps:

A. Partitioning into subdomains

B. Selection of the wave functions in the pressure expansion

C. Construction of the system of equations via a weighted residual formulation of the boundary and continuity conditions

D. Solution of the system of equations and postprocessing of the dynamic variables

3.1 Partitioning into subdomains

When applied for bounded problems, a sufficient condition for the WB approximations to converge towards the exact solution, is convexity of the considered problem domain [Desmet (1998)]. In a general acoustic problem, the acoustic problem domain may be non-convex so that a partitioning into a number of convex subdomains is required.

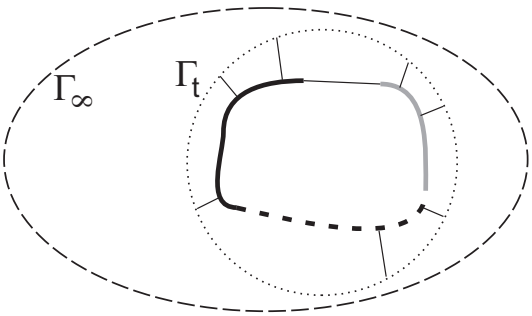

Figure 2: A WB partitioning of the unbounded problem

If the WBM is applied for unbounded problems, an initial partitioning of the unbounded domain into a bounded and an unbounded region precedes the partitioning

into convex subdomains [Pluymers, Van Hal, Vandepitte, and Desmet (2007)]. Figure 2 illustrates the principle. The entire acoustic problem domain is divided into two non-overlapping regions by a spherical truncation surface Γ_t. The unbounded region exterior to Γ_t is considered as one acoustic subdomain.

3.2 Acoustic pressure expansion

The steady-state acoustic pressure field $p^{(\alpha)}(\underline{r})$ in a (bounded or unbounded) acoustic subdomain $\Omega^{(\alpha)}$ ($\alpha = 1 \ldots N_\Omega$, with N_Ω the number of subdomains) is approximated by a solution expansion $\hat{p}^{(\alpha)}(\underline{r})$:

$$\begin{aligned} p^{(\alpha)}(\underline{r}) \simeq \hat{p}^{(\alpha)}(\underline{r}) &= \sum_{w=1}^{n_w^{(\alpha)}} {p_w}^{(\alpha)} \Phi_w^{(\alpha)}(\underline{r}) + \hat{p}_f^{(\alpha)}(\underline{r}) \\ &= \underline{\Phi}^{(\alpha)}(\underline{r})\, \underline{{p_w}}^{(\alpha)} + \hat{p}_f^{(\alpha)}(\underline{r}) \end{aligned} \tag{7}$$

The $n_w^{(\alpha)}$ wave function contributions $p_w^{(\alpha)}$ are the weighting factors for each of the selected wave functions $\Phi_w^{(\alpha)}$. Together they form the vector of degrees of freedom $\underline{{p_w}}^{(\alpha)}$. The corresponding *a priori* defined wave functions are collected in the row vector $\underline{\Phi}^{(\alpha)}$. The set of all $n_W = \sum_{\alpha=1}^{N_\Omega} n_w^{(\alpha)}$ acoustic wave function contributions p_w is collected in the column vector $\underline{p_w}$, while the row vector $\underline{\Phi}$ contains all n_W wave functions. $\hat{p}_f^{(\alpha)}$ represents a particular solution resulting from acoustic source terms $\mathscr{F}^{(\alpha)}$ in the right hand side of the inhomogeneous Helmholtz equation (1).

3.2.1 Wave functions for a bounded subdomain

Each acoustic wave function $\Phi_w^{(\alpha)}(\underline{r})$ exactly satisfies the homogeneous Helmholtz equation (1). For 3D bounded subdomains three types of wave functions are distinguished, the r-, s- and t-set:

$$\sum_{w=1}^{n_w^{(\alpha)}} {p_w}^{(\alpha)} \Phi_w^{(\alpha)}(\underline{r}) = \sum_{w_r=1}^{n_{w_r}^{(\alpha)}} {p_{w_r}}^{(\alpha)} \Phi_{w_r}^{(\alpha)}(\underline{r}) + \sum_{w_s=1}^{n_{w_s}^{(\alpha)}} {p_{w_s}}^{(\alpha)} \Phi_{w_s}^{(\alpha)}(\underline{r}) + \sum_{w_t=1}^{n_{w_t}^{(\alpha)}} {p_{w_t}}^{(\alpha)} \Phi_{w_t}^{(\alpha)}(\underline{r}), \tag{8}$$

with $n_w^{(\alpha)} = n_{w_r}^{(\alpha)} + n_{w_s}^{(\alpha)} + n_{w_t}^{(\alpha)}$. These wave functions are defined as:

$$\Phi_w^{(\alpha)}(\underline{r}\,(x,y,z)) = \begin{cases} \Phi_{w_r}^{(\alpha)}(x,y,z) = \cos(k_{xw_r}^{(\alpha)} x)\cos(k_{yw_r}^{(\alpha)} y)\, e^{-jk_{zw_r}^{(\alpha)} z} \\ \Phi_{w_s}^{(\alpha)}(x,y,z) = \cos(k_{xw_s}^{(\alpha)} x)\, e^{-jk_{yw_s}^{(\alpha)} y}\cos(k_{zw_s}^{(\alpha)} z) \\ \Phi_{w_t}^{(\alpha)}(x,y,z) = e^{-jk_{xw_t}^{(\alpha)} x}\cos(k_{yw_t}^{(\alpha)} y)\cos(k_{zw_t}^{(\alpha)} z) \end{cases} \tag{9}$$

The only requirement for the wave functions (9) to be exact solutions of (1) is

$$\begin{aligned} & \left(k_{xw_r}^{(\alpha)}\right)^2 + \left(k_{yw_r}^{(\alpha)}\right)^2 + \left(k_{zw_r}^{(\alpha)}\right)^2 \\ = & \left(k_{xw_s}^{(\alpha)}\right)^2 + \left(k_{yw_s}^{(\alpha)}\right)^2 + \left(k_{zw_s}^{(\alpha)}\right)^2 \\ = & \left(k_{xw_t}^{(\alpha)}\right)^2 + \left(k_{yw_t}^{(\alpha)}\right)^2 + \left(k_{zw_t}^{(\alpha)}\right)^2 \quad = k^2. \end{aligned} \tag{10}$$

As a result, an infinite number of wave functions (9) can be defined for expansion (7). Desmet (1998) proposes to select the following wave number components:

$$\begin{cases} \left(k_{xw_r}^{(\alpha)}, k_{yw_r}^{(\alpha)}, k_{zw_r}^{(\alpha)}\right) = \left(\frac{w_1^{(\alpha)}\pi}{L_x^{(\alpha)}}, \frac{w_2^{(\alpha)}\pi}{L_y^{(\alpha)}}, \pm\sqrt{(k)^2 - \left(k_{xw_r}^{(\alpha)}\right)^2 - \left(k_{yw_r}^{(\alpha)}\right)^2}\right) \\ \left(k_{xw_s}^{(\alpha)}, k_{yw_s}^{(\alpha)}, k_{zw_s}^{(\alpha)}\right) = \left(\frac{w_3^{(\alpha)}\pi}{L_x^{(\alpha)}}, \pm\sqrt{(k)^2 - \left(k_{xw_s}^{(\alpha)}\right)^2 - \left(k_{zw_s}^{(\alpha)}\right)^2}, \frac{w_4^{(\alpha)}\pi}{L_z^{(\alpha)}}\right) \\ \left(k_{xw_t}^{(\alpha)}, k_{yw_t}^{(\alpha)}, k_{zw_t}^{(\alpha)}\right) = \left(\pm\sqrt{(k)^2 - \left(k_{yw_t}^{(\alpha)}\right)^2 - \left(k_{zw_t}^{(\alpha)}\right)^2}, \frac{w_5^{(\alpha)}\pi}{L_y^{(\alpha)}}, \frac{w_6^{(\alpha)}\pi}{L_z^{(\alpha)}}\right) \end{cases} \tag{11}$$

with $w_1^{(\alpha)} \ldots w_6^{(\alpha)} = 0, 1, 2, \ldots$. The dimensions $L_x^{(\alpha)}$, $L_y^{(\alpha)}$ and $L_z^{(\alpha)}$ represent the dimensions of the (smallest) bounding box, circumscribing the considered subdomain.

3.2.2 Wave functions for an unbounded subdomain

The wave functions for the unbounded domain are chosen to implicitly obey the Sommerfeld radiation condition (6). This removes the need to explicitly impose a radiation condition, similar to the BEM. The following multipole series is proposed as a wave function set for 3D unbounded problems based on [Ihlenburg (1998)]:

$$\Phi_{uv}^{(ub)}(\underline{r}(r,\theta,\phi)) = h_u^{(2)}(kr) Y_u^v(\theta,\phi). \tag{12}$$

In this expression, $h_u^{(2)}(kr)$ is the spherical Hankel function of the second kind:

$$h_u^{(2)}(kr) = \sqrt{\frac{\pi}{2kr}} H_{u+1/2}^{(2)}(kr), \tag{13}$$

and $Y_u^v(\theta,\phi)$ are the spherical harmonics:

$$Y_u^v(\theta,\phi) = \sqrt{\frac{2u+1}{4\pi}\frac{(u-v)!}{(u+v)!}} P_w^v(\cos(\theta))\, e^{jv\phi}, \tag{14}$$

with $P_u^v(\cdot)$ the associated Legendre function of order u and degree v. For each order $u = 1, 2, \ldots u_{max}$, the corresponding degrees $v = -u \ldots u$ are included in the function set, yielding a total of $n_w^{(\alpha)} = (u_{max}+1)^2$ wave functions.

3.2.3 Source formulations

For modeling sources in both bounded and unbounded acoustic domains, a particular solution representing free field pressure of the desired source is required. Similar as in Bergen, Pluymers, Van Genechten, Vandepitte, and Desmet (2010), particular solution terms are derived for point source and plane wave excitation. For an acoustic point source, the particular solution term yields:

$$\hat{p}_f^{(\alpha)}(x,y,z) = \quad Q^{(\alpha)} \frac{e^{-jkr_q^{(\alpha)}}}{r_q^{(\alpha)}} \quad . \tag{15}$$

with $r_q^{(\alpha)} = \sqrt{(x-x_q^{(\alpha)})^2 + (y-y_q^{(\alpha)})^2 + (z-z_q^{(\alpha)})^2}$ for a source at position $(x_q^{(\alpha)}, y_q^{(\alpha)}, z_q^{(\alpha)})$ and $Q^{(\alpha)}$ the source strength.
Another commonly used excitation is a plane wave source (in an unbounded problem). For this source, the particular solution term yields:

$$\hat{p}_f(x,y,z) = Q_{pw} e^{jk\left(\underline{d}(r_{pw})\right)} \ , \tag{16}$$

with Q_{pw} the plane wave amplitude and $\underline{d}(r_{pw})$ the propagation vector.

3.3 Acoustic wave model

The proposed expansion functions (9) and (12) exactly satisfy the (homogeneous part of the) Helmholtz equation (1) inside the domain and, in the case of the unbounded function set (12), also the Sommerfeld radiation condition (6). The boundary conditions and subdomain continuity are enforced through a weighted residual formulation. The residuals on the boundary conditions are given in (3), (4) and (5), and the residuals enforcing continuity between two subdomains α and β can be written as

$$\underline{r} \in \Gamma_I : R_I^{(\alpha,\beta)} = \left(\frac{j}{\rho_0 \omega} \frac{\partial p^{(\alpha)}(\underline{r})}{\partial n^{(\alpha)}} - \frac{p^{(\alpha)}}{\overline{Z}_{int}}\right) + \left(\frac{j}{\rho_0 \omega} \frac{\partial p^{(\beta)}(\underline{r})}{\partial n^{(\beta)}} + \frac{p^{(\beta)}}{\overline{Z}_{int}}\right) , \tag{17}$$

with $n^{(\alpha)}$ the local normal on the interface, outwards of domain α and $\overline{Z}_{int}$ an impedance coupling factor, chosen as $\rho_0 c$ [Pluymers (2006)].

For each subdomain, the error functions are orthogonalized with respect to a weighting function $\tilde{p}^{(\alpha)}$ or its derivative. The weighted residual formulation, applying the introduced error functions, is expressed as:

$$\int_{\Gamma_v^{(\alpha)}} \tilde{p}^{(\alpha)}(\underline{r})\, R_v^{(\alpha)}(\underline{r}) \mathrm{d}\Gamma + \int_{\Gamma_Z^{(\alpha)}} \tilde{p}^{(\alpha)}(\underline{r})\, R_Z^{(\alpha)}(\underline{r}) \mathrm{d}\Gamma$$
$$+ \int_{\Gamma_p^{(\alpha)}} -\mathscr{L}_v^{(\alpha)}(\tilde{p}^{(\alpha)}(\underline{r}))\, R_p^{(\alpha)}(\underline{r}) d\Gamma + \sum_{\beta=1,\beta\neq\alpha}^{N_\Omega} \int_{\Gamma_I^{(\alpha,\beta)}} \tilde{p}^{(\alpha)}(\underline{r})\, R_I^{(\alpha,\beta)}(\underline{r}) \mathrm{d}\Gamma = 0.$$

(18)

Like in the Galerkin weighting procedure, used in the FEM, the weighting functions $\tilde{p}^{(\alpha)}$ are expanded in terms of the same set of acoustic wave functions used in the pressure expansion (7):

$$\tilde{p}^{(\alpha)}(\underline{r}) = \sum_{a=1}^{n_w^{(\alpha)}} \tilde{p_a}^{(\alpha)} \Phi_a^{(\alpha)}(\underline{r}) = \underline{\Phi}^{(\alpha)}(\underline{r})\, \underline{\tilde{p}_w}^{(\alpha)}. \tag{19}$$

Substitution of the pressure expansion (7) and the weighting function expansion (19) into the weighted residual formulation (18) yields a set of $n_w^{(\alpha)}$ linear equations in the n_W unknown wave function contribution factors. One such matrix equation is obtained for each subdomain. Combination of the N_Ω systems yields the acoustic WB model, consisting of n_W algebraic equations in the n_W unknown wave function contribution factors:

$$\left[\ A\ \right] \left\{\ \underline{p_w}\ \right\} = \left\{\ \underline{b}\ \right\}. \tag{20}$$

3.4 Solution and postprocessing

The resulting model (20) can be solved for the unknown wave function contributions p_w. The final step in the modeling process is backsubstitution of these contribution factors into the pressure expansions (7), yielding an analytical description of the approximated dynamic pressure field $\hat{p}(\underline{r})$.

3.5 WBM model properties

Where the FEM and BEM use simple polynomials in a fine discretization to describe the dynamic variables, the WBM uses wave functions in a coarse partitioning of the domain. As a consequence, the WBM does not suffer from pollution errors and relatively few degrees of freedom are needed to accurately represent the dynamic field. The downside of this is the requirement of convex subdomains (for the bounded domains), deteriorating the efficiency when the problem geometry is complex and extensive partitioning is needed.

Derived quantities like acoustic velocity and intensity can be easily calculated from the analytic derivatives of the basis functions. Because of the wave-like nature of those basis functions, there is no loss of accuracy for derived variables, since the derivatives are also analytical functions with a similar spatial resolution.

The use of a Trefftz basis typically leads to ill-conditioned systems [Tsai, Lin, Young and Atluri (2006); Liu, Yeih and Atluri (2009)]. Therefore, the highly oscillatory integrals (18) should be evaluated with care to ensure the matrix coefficients

are are determined to high accuracy. The use of a Gauss-Legendre quadrature with a fixed number of integration points per wavelength allows an efficient integration meeting the desired accuracy. Furthermore, Desmet (1998) proves that the system resulting from a WB model meets the so-called Picard conditions [Varah (1979)], indicating an accurate solution can be obtained despite the unfavorable condition number. The results of similar Picard tests performed for the 3D unbounded numerical examples presented here support the observations made by Desmet (1998) and hence indicate that the introduction of the proposed set of unbounded basis functions in the WBM approach does not adversely affect the practical convergence of the method.

As for the BE method and in contrast with the FE method, the WBM yields a fully populated matrix, whose elements are complex and which cannot be decomposed into frequency independent submatrices. However, because the system is substantially smaller, the computation times are generally much shorter as compared to the element-based methods. These advantageous computation times, combined with the good accuracy of the WBM, result in an excellent convergence rate and a computational efficiency which is superior to the FEM and BEM for a wide range of steady-state dynamic problems [Vanmaele, Vandepitte, and Desmet (2009); Desmet, Van Hal, Sas, and Vandepitte (2002); Pluymers, Desmet, Vandepitte, and Sas (2005)], allowing the method to tackle problems at higher frequencies.

4 Numerical examples

This section discusses two numerical examples. In a first example, the proposed formulations are verified by comparison with an analytical solution. The problem considered is the scattering of a plane wave on an acoustically rigid or soft sphere. A second example studies the scattering of the so-called cat's eye problem [Makarov and Ochmann (1997)].

4.1 3D Scattering problem: rigid sphere

The acoustic scattering of a plane wave, incident along the negative Z-axis on both a rigid and sound-soft ($\overline{p} = 0$) sphere with radius 1m is considered. The acoustic fluid is air ($c = 340$ m/s, $\rho_0 = 1.225$ kg/m^3). A reference solution for this problem is available in the form of a series expansion [Makarov and Ochmann (1997)]:

$$p_s(r,\theta) = p_0 \sum_n D_n h_n^{(2)}(kr) P_n(\cos\theta), \tag{21}$$

with (r,θ) the spherical coordinates of the observation point. Due to the symmetry of the problem, the scattered field does not depend on the azimuthal angle ϕ. The

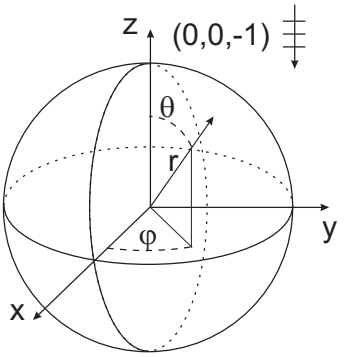

Figure 3: geometry and source definition

coefficients D_n in (21) can be calculated as:

$$D_n = p_0(2n+1)j^n \frac{n\mathscr{J}_{n-1}(kR_0) - (n+1)\mathscr{J}_{n+1}(kR_0)}{nh_{n-1}^{(2)}(kR_0) - (n+1)h_{n+1}^{(2)}(kR_0)} \quad \text{for a rigid sphere} \tag{22}$$

$$D_n = p_0(2n+1)j^n \frac{n\mathscr{J}_n(kR_0)}{nh_n^{(2)}(kR_0)} \quad \text{for a soft sphere} \tag{23}$$

$\mathscr{J}_n$ is the spherical bessel function:

$$\mathscr{J}_n(x) = \sqrt{\frac{\pi}{2x}} J_{n+1/2}(x), \tag{24}$$

with J_n the Bessel function of the first kind and order n.

This reference solution will allow for a thorough evaluation of the accuracy of the proposed method, where a BE model of the same problem enables to assess the computational efficiency.

The WB model consists of a single unbounded subdomain, and is refined by adding wave functions in the pressure expansion (7). The details of the BE models constructed for the numerical comparison are listed in table 1.

Figure 4 shows the directivity of the pressure field at a radius of 2m, both for the case with a rigid sphere as with a soft sphere. The analytic solution of the problem is plotted along as a reference, indicating an excellent agreement with the result obtained using the WBM.

To assess the accuracy and computational efficiency, the average relative error in 70 points around the sphere is calculated for BE and WB models of increasing size. Sysnoise rev. 5.6 is used as solver for the BE models. All calculations are

Table 1: BEM model information for the rigid sphere. * maximum frequency with 6 or 10 elements per wavelength throughout the mesh [Bouillard and Ihlenburg (1999)]

	element size	♯ DOF	mesh validity: * 6 el./ λ [Hz]	10 el./λ [Hz]	calculation time [s]
BEM	100*mm*	2910	381	229	2.67
	75*mm*	5016	500	300	7.31
	50*mm*	11068	763	458	49
	37*mm*	19430	931	559	226
	25*mm*	43360	1410	846	2225

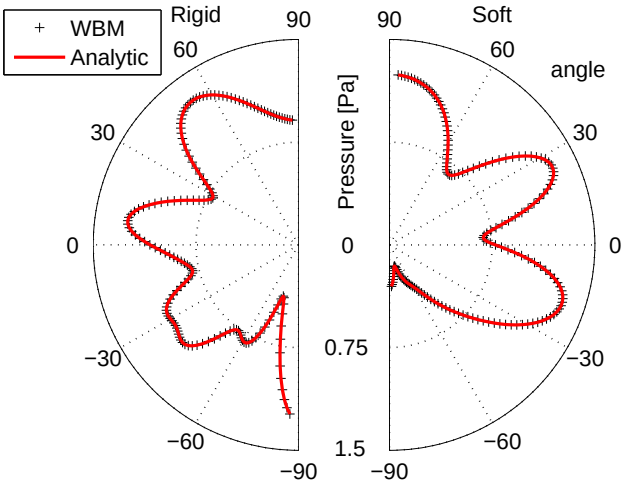

Figure 4: Pressure amplitude [Pa] directivity at 2m for the rigid (left) and soft (right) sphere

carried out on an intel Xeon 5355 based system with 32 GB memory running a linux operating system. The resulting convergence graphs, relating prediction accuracy to computational cost (CPU time), are shown in figure 5 (rigid sphere) and 6 (soft sphere) for 3 frequencies between 250 and 640 Hz ($ka \simeq 10...25$). It is clear that the WBM result converges very fast to the analytic solution, indicating both the good prediction accuracy and the efficiency potential of the proposed approach. BEM convergence, in comparison, is much slower, which is particulary pronounced for this geometrically simple problem.

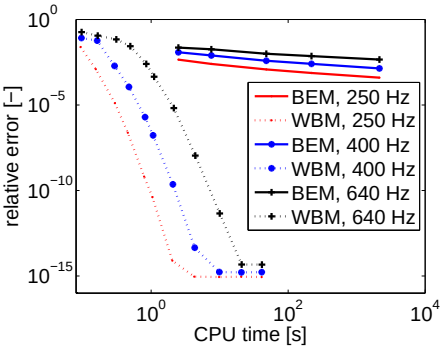

Figure 5: Convergence diagram, WBM vs. BEM: rigid sphere

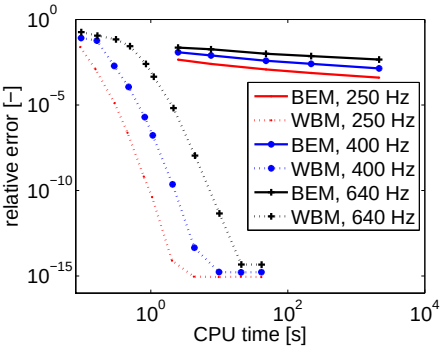

Figure 6: Convergence diagram, WBM vs. BEM: soft sphere

4.2 3D Scattering problem: cat's eye

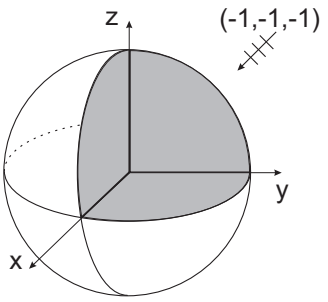

Figure 7: geometry of the cat's eye problem

A second case considers the acoustic scattering of the cat's eye problem [Makarov and Ochmann (1997)]. The cat's eye consists of a rigid sphere of radius 1m with the positive octant cut out, as shown in figure 7. The system is excited by an incident plane wave traveling along the centerline of the positive octant (propagation direction (-1,-1,-1)). The acoustic fluid is air ($c = 340$ m/s, $\rho_0 = 1.225$ kg/m^3). The WB model consists of one bounded (the cut-out) and one unbounded subdomain. Several BEM models are constructed for a numerical comparison, the details are listed in table 2.

Figures 8 and 9 show the acoustic pressure field (amplitude) and the relative error of this pressure field, respectively. The relative error is well below 1% throughout the domain and is only slightly larger at the pressure nodal lines, where the relative error is most sensitive to small variations.

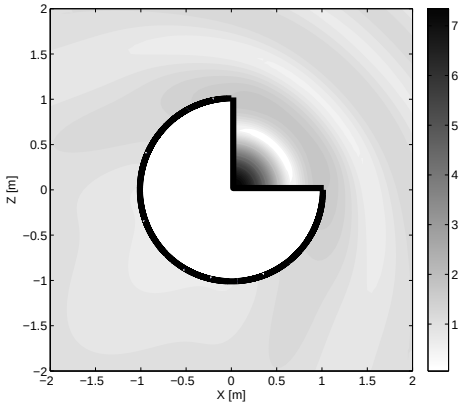

Figure 8: Acoustic Pressure Amplitude [Pa] in xz plane, 250Hz ($ka \simeq 10$)

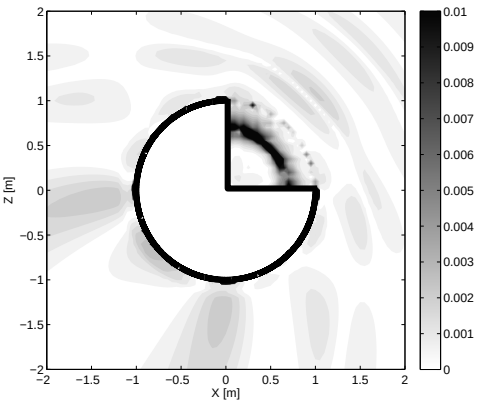

Figure 9: Pressure Amplitude relative prediction error [-] in xz plane, 250Hz ($ka \simeq 10$)

Also for this second validation example, a convergence calculation is carried out. The resulting convergence graph is shown in figure 10. It can be observed that the advantageous convergence rate observed in the previous case is well conserved in this more complicated problem. While the level of the relative error is in this case constrained by the obtainable accuracy of the BE reference model, it is clear that convergence to this accuracy is substantially faster using a WB model as compared to a BEM prediction. In this case, it can be concluded that the WBM is $\approx$100 times faster compared to the BEM for a similar accuracy.

The improved efficiency of the WBM enables accurate predictions in a wider fre-

Table 2: BEM model information for the cat's eye. * maximum frequency with 6 or 10 elements per wavelength throughout the mesh [Bouillard and Ihlenburg (1999)]

	element size	♯ DOF	mesh validity: * 6 el./ λ [Hz]	10 el./λ [Hz]	calculation time [s]
BEM	100mm	3240	381	229	3.18
	75mm	5692	500	300	10.27
	50mm	12250	763	458	71.6
	37mm	21438	931	559	299
	25mm	46216	1410	846	2885
ref.	18mm	88126	1992	1196	/

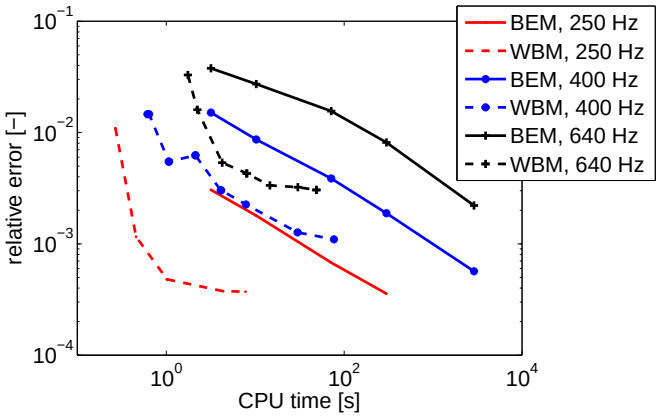

Figure 10: Convergence diagram, WBM vs. BEM ($ka \simeq 10...25$)

quency range as compared to the BEM. This can be clearly observed when looking at frequency response predictions. In figure 11, the pressure amplitude Frequency Response Function (FRF) is shown, calculated both with the BE model with 100mm mesh size (left), and with the WBM (right). The prediction obtained using a fine BE model (25mm) is plotted as reference. As predicted by the rule-of-thumb (using 6 elements/λ), the BEM prediction accuracy starts to deteriorate around 400 Hz. A WB model of similar calculation time, however, retains excellent accuracy throughout a much larger frequency range.

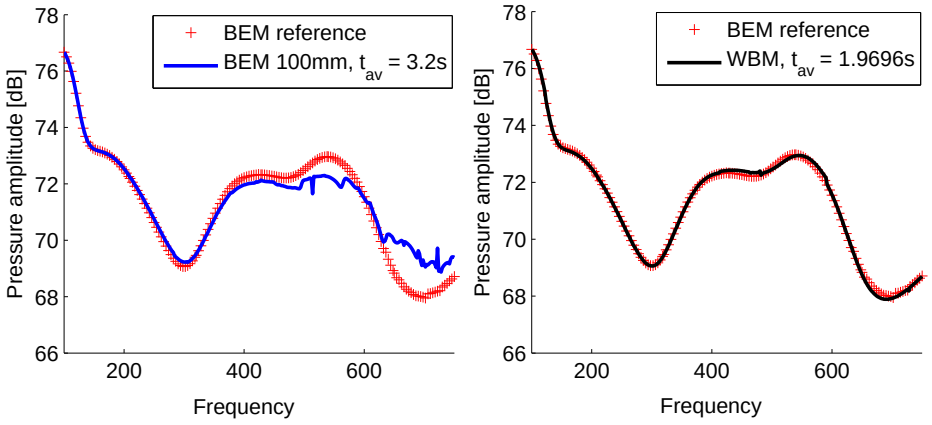

Figure 11: Pressure amplitude FRF [dB re $2e^{-5}$Pa] comparison

5 Conclusions

This paper presents the extension of the Wave Based Method (WBM) for the treatment of 3D acoustic problems in unbounded domains. First, the problem is separated into a bounded and an unbounded part. To efficiently model the unbounded part, a function set is needed that not only satisfies the Helmholtz equation, but also the Sommerfeld radiation condition. A suitable function set is proposed, together with a formulation for two common sources in scattering problems: a point source and an incident plane wave.

The prediction accuracy and computational efficiency of the proposed approach are validated on two numerical examples: the scattering of a plane wave by a rigid or soft sphere and the cat's eye problem. In both cases, it is shown that the convergence rate is strongly improved as compared to the BE method. This enhanced computational efficiency allows to apply the WBM for problems in an extended frequency range.

Acknowledgement: The research of Bart Bergen is funded by a Ph.D. grant of the Institute for the Promotion of Innovation through Science and Technology in Flanders (IWT-Vlaan-deren) and Bert Van Genechten is a doctoral fellow of the Research Foundation Flanders (FWO), Belgium. Furthermore, the authors gratefully acknowledge the European commision for their support of the ITN Marie Curie project GA-214909 "MIDFREQUENCY - CAE Methodologies for Mid-Frequency Analysis in Vibration and Acoustics.

References

Bergen, B.; Pluymers, B.; Van Genechten, B.; Vandepitte, D.; Desmet, W. (2010): A Trefftz based method for solving Helmholtz problems in semi-infinite domains. *submitted to Journal of Computational and Applied Mathematics*.

Bettess, P. (1992): *Infinite Elements*. Penshaw Press.

Bettess, P. (2004): Short-wave scattering: problems and techniques. *Philosophical Transactions of the Royal Society A, London*, pp. 421–443.

Bleszynski, E.; Bleszynski, M.; Jaroszewicz, T. (2004): Development of New Algorithms for High Frequency Electromagnetic Scattering. *CMES: Computer Modeling in Engineering & Sciences*, vol. 5, pp. 295–318.

Bouillard, P.; Ihlenburg, F. (1999): Error estimation and adaptivity for the finite element method in acoustics: 2D and 3D applications. *Computer Methods in Applied Mechanics and Engineering*, vol. 176, pp. 147–163.

Callsen, S.; Von Estorff, O.; Zaleski, O. (2004): Direct and indirect approach of a desingularized boundary element formulation for acoustical problems. *CMES: Computer Modeling in Engineering & Sciences*, vol. 6, pp. 421–430.

Chandler-Wilde, S. N.; Graham, I. G. (2009): Boundary integral methods in high-frequency scattering. *University of Reading Math Preprint series 2008/09. from:* Highly oscillatory problems: computation, theory and applications. *Cambridge, Cambridge University Press; 2008.*

Cho, H. A., Golberg, M. A.; Muleshkov, A. S.; Li, X. (2004): Trefftz methods for time dependent partial differential equations. *CMC: Computers, Materials & Continua*, vol. 1, pp. 1- 37.

Desmet, W. (1998): *A wave based prediction technique for coupled vibro-acoustic analysis*. KULeuven, division PMA, PhD. thesis 98D12, `http://www.mech.kuleuven.be/mod/wbm/phd_dissertations`.

Desmet, W.; Van Hal, B.; Sas, P.; Vandepitte, D. (2002): A computationally efficient prediction technique for the steady-state dynamic analysis of coupled vibro-acoustic systems. *Advances in Engineering Software*, vol. 33, pp. 527–540.

Givoli, D (2008): Computational absorbing boundaries. *Computational Acoustics of Noise Propagation in Fluids.* S. Marburg and B. Nolte, eds., Chapter 5, pp. 145-166, Berlin, Springer, 2008.

Glassner, A. S.(Ed): *An introduction to ray tracing*. Academic Press Ltd., London, UK, UK.

Harari, I. (2006): A survey of finite element methods for time-harmonic acoustics. *Computer Methods in Applied Mechanics and Engineering*, vol. 195, pp. 1594–1607.

He, X.; Lim, K.-M.; Lim, S.-P. (2008): Fast BEM Solvers for 3D Poisson-type equations. *CMES: Computer Modeling in Engineering & Sciences*, vol. 35, pp. 21–48.

Huybrechs, D.; Vandewalle, S. (2006): On the evaluation of highly oscillatory integrals by analytic continuation. *SIAM Journal on Numerical Analysis*, pp. 1026–1048.

Ihlenburg, F. (1998): *Finite element analysis of acoustic scattering*. Volume 132 of Applied Mathematical Sciences, Springer.

Liu, C.-S.; Yeih, W.; Atluri, S.N. (2009): On solving the ill-conditioned system Ax = b: general-purpose conditioners obtained from the boundary-collocation solution of the Laplace equation, using Trefftz expansions with multiple length scales. *CMES: Computer Modeling in Engineering & Sciences*, vol.44, no.3, pp.281-311.

Li, Z. C.; Lu, T. T.; Huang, H. T.; Cheng, A. H. D. (2007): Trefftz, collocation, and other boundary methods - A comparison. *Num. Meth. Par. Diff. Eq.*, vol. 23, pp. 93-144.

Lu, Y. Y.; Zhu, J. (2007): Perfectly matched layer for acoustic waveguide modeling - benchmark calculations and perturbation analysis. *CMES: Computer Modeling in Engineering & Sciences*, vol. 22, pp. 235–148.

Makarov, S. N.; Ochmann, M. (1997): An iterative solver of the Helmholtz integral equation for high-frequency acoustic scattering. *Journal of the Acoustical Society of America*, vol. 103, pp. 742–750.

Marburg, S. (2002): Six boundary elements per wavelength: is that enough? *Journal of Computational Acoustics*, vol. 10, pp. 25–51.

Patlashenko, I.; Givoli, D. (2000): Numerical solution of nonlinear exterior wave problems using local absorbing boundary conditions. *CMES: Computer Modeling in Engineering & Sciences*, vol. 1, pp. 61–70.

Pluymers, B. (2006): *Wave based modelling methods for steady-state vibroacoustics*. KULeuven, division PMA, PhD. thesis 2006D04, `http://www.mech.kuleuven.be/mod/wbm/phd_dissertations`.

Pluymers, B.; Desmet, W.; Vandepitte, D.; Sas, P. (2005): On the use of a wave based prediction technique for steady-state structural-acoustic radiation analysis. *CMES: Computer Modeling in Engineering & Sciences*, vol. 7, no. 2, pp. 173–184.

Pluymers, B.; Van Hal, B.; Vandepitte, D.; Desmet, W. (2007): Trefftz-based methods for time-harmonic acoustics. *Archives of Computational Methods in Engineering*. vol. 14, no. 4, pp. 343-389.

Qian, Z.; Han, Z.; Ufimtsev, P.; Atluri, S. (2004): Non-hyper-singular boundary integral equations for acoustic problems, implemented by the collocation-based boundary element method. *CMES: Computer Modeling in Engineering & Sciences*, vol. 6, pp. 133–144.

Sas, P.; Desmet, W.; Vandepitte, D. (1998): A wave-based prediction technique for vibroacoustics: Comparison with the finite-element technique and experimental validation. *Journal of the Acoustical Society of America*, vol. 103, pp. 2770.

Sladek, J.; Sladek, V.; Kompis, V.; Van Keer, R. (2000): Application of multiregion Trefftz method to elasticity. *CMES: Computer Modeling in Engineering & Sciences*, vol.1, no.4, pp.1-8.

Takei, A.; Yoshimura, S.; Kanayama, H. (2009): Large-scale full wave analysis of electromagnetic field by hierarchical domain decomposition method. *CMES: Computer Modeling in Engineering & Sciences*, vol. 40, pp. 63–82.

Thompson, L. L. (2006): A review of finite element methods for time-harmonic acoustics. *Journal of the Acoustical Society of America*, vol. 119, pp. 1315–1330.

Trefftz, E. (1926): Ein Gegenstück zum Ritzschen Verfahren. In *Proceedings of the 2nd International Congress on Applied Mechanics, Zurich, Switzerland*, pp. 131–137.

Trevelyan, J.; Coates, G. (2010): On adaptive definition of the plane wave basis for wave boundary elements in acoustic scattering: the 2D case. *CMES: Computer Modeling in Engineering & Sciences*, vol.55, no.2, pp.147-168.

Tsai, C. C.; Lin, Y. C.; Young, D. L.; Atluri, S. N. (2006): Investigations on the accuracy and condition number for the method of fundamental solutions. *CMES: Computer Modeling in Engineering & Sciences*, vol. 16, pp. 103-114.

Van Genechten, B.; Bergen, B.; Vandepitte, D.; Desmet, W. (2010): A Trefftz-based numerical modelling framework for Helmholtz problems with complex multiple-scatterer configurations. *Journal of Computational Physics* vol. 229, no. 18, pp. 6623-6643.

Van Genechten, B.; Vergote, K.; Vandepitte, D.; Desmet, W. (2010): A multi-level wave based numerical modelling framework for the steady-state dynamic analysis of bounded helmholtz problems with multiple inclusions. *Computer Methods in Applied Mechanics and Engineering*, vol. 199, no. 29-32, pp. 1881-1905.

Van Genechten, B.; Vandepitte, D.; Desmet, W. (2010): A direct hybrid finite element - wave based modelling technique for efficient mid-frequency coupled vibro-acoustic analysis. *Computer Methods in Applied Mechanics and Engineering*, under consideration.

Vanmaele, C.; Vandepitte, D.; Desmet, W. (2007): An efficient wave based prediction technique for plate bending vibrations. *Computer Methods in Applied Mechanics and Engineering*, vol. 196, pp. 3178 – 3189.

Vanmaele, C.; Vandepitte, D.; Desmet, W. (2009): An efficient wave based prediction technique for dynamic plate bending problems with corner stress singularities. *Computer Methods in Applied Mechanics and Engineering*, vol. 198, no. 30-32, pp. 2227 – 2245.

Varah, J.M. (1979): A practical examination of some numerical methods for linear discrete ill-posed problems. *SIAM Review*, vol. 21, pp. 100-111.

Von Estorff, O. (2000): *Boundary elements in acoustics: advances and applications*. WITpress.

Young, D. L.; Ruan J. W. (2005): Method of fundamental solutions for scattering problems of electromagnetic waves. *CMES: Computer Modeling in Engineering & Sciences*, vol. 7, pp. 223- 232.

Yue, B.; Guddati, M. N. (2005): Dispersion-reducing finite elements for transient acoustics. *Journal of the Acoustical Society of America*, vol. 118, pp. 2132-2141.

Zienkiewicz, O. C.; Taylor, R. L.; Zhu, J. Z. (2005): *The finite element method - vol. 1: its basis & fundamentals*. Butterworth-Heinemann, 6th edition.